Mon. Not. R. Astron. Soc. **000**, 000–000 (0000) Printed 9 February 2022 (MN LATEX style file v2.2)

Rapid variability in TeV blazars: the case of PKS 2155–304

G. Ghisellini[1⋆], F. Tavecchio[1]
[1]*INAF – Osservatorio Astronomico di Brera, Via E. Bianchi 46, I-23807 Merate, Italy*

9 February 2022

arXiv:0801.2569v2 [astro-ph] 6 Feb 2008

ABSTRACT
Recent Cherenkov observations of BL Lac objects showed that the TeV flux of PKS 2155–304 changed by a factor 2 in just 3–5 minutes. This fast variability can be accounted for if the emitting region is moving with a bulk Lorentz factor $\Gamma \sim 50$ and a similar relativistic Doppler factor. If this Γ is adopted, several models can fit the data, but, irrespective of the chosen model, the jet is matter dominated. The Doppler factor requires viewing angles of the order of 1° or less: if the entire jet is as narrow as this, then we have problems with current unification schemes. This suggests that there are small active regions, inside a larger jet, moving faster than the rest of the plasma, occasionally pointing at us. Coordinated X–ray/TeV variability can discriminate between the different scenarios.

Key words: radiation mechanisms: general — galaxies: active — BL Lacertae objects: individual: PKS 2155–304 — galaxies: jets — gamma-rays: observations

1 INTRODUCTION

The blazars PKS 2155–304 (Aharonian et al. 2007) and Mkn 501 (Albert et al. 2007) showed variations on $t_{\rm var}$ =3–5 minutes of their TeV flux. This ultrafast variability calls for a revision of our current ideas about the properties of the emitting region. Particularly challenging is the case of PKS 2155–304, because the variations occurred during an overall very active state of the source with an observed TeV luminosity of $\sim 10^{47}$ erg s^{-1}. The usual way to infer the size from the variability timescale is $R < ct_{\rm var}\delta$ where δ is the Doppler factor. Begelman, Fabian & Rees (2008; hereafter B08) pointed out that such small $t_{\rm var}$ cannot be any longer indicative of the size of the black hole (as instead are in the "internal shock scenario" (Sikora et al 1994, Ghisellini 1999, Spada et al. 2001, Guetta et al. 2004). The mass of the central black hole of PKS 2155–304 is uncertain (of the order of 10^9 $M_\odot$; Aharonian et al. 2007) but even a (prudently small) mass of $M = 10^8$ solar masses corresponds to a light travel time across the Schwarzschild radius of 10^3 s. To avoid to have a too compact source, with the accompanying problem of γ–ray absorption through the γ–$\gamma \to e^\pm$ process (see e.g. Dondi & Ghisellini 1995), the bulk Lorentz factor of the emitting region (hence δ) must have a value close to 50. This requirement is not unprecedented, since also the large separation, in frequency, of the two broad peaks characterising the spectral energy distribution (SED) requires $\delta > 30$ in single–zone synchrotron self Compton (SSC) models (see e.g. Konopelko et al. 2003). Smaller δ and Γ factors are however possible in alternative models, where two or more emission regions have different Γ, as in the decelerating jet model of Georganopoulos & Kazanas (2003) and in the "spine–layer" model proposed by Ghisellini, Tavecchio & Chiaberge (2005; hereafter G05). In both models contiguous emitting regions of the jet are moving with different Γ, and one part can see the emission of other relativistically boosted, thus enhancing the radiation energy density and the consequent inverse Compton emission. In this way one can relax the requirement of having Γ–factors of the order of 30 or more, requiring a more standard value of around 15. The observed rapid variability, instead, cannot be "cured" by invoking a structured jet emission region, and is therefore more demanding.

The implied large Γ makes any external photon source strongly boosted in the comoving frame, favouring the "external Compton" (EC) process, in which the energy density of the seed photons produced outside the jet is larger than the energy density of the synchrotron radiation produced locally. This argument leads B08 to suggest that the EC process is the main radiation mechanism. They also argue that, since to produce TeV photons one needs highly energetic electrons (with random Lorentz factors $\gamma \sim 10^6/\Gamma$), the jet could be particle starved (i.e. one needs fewer electrons to produce the radiation we see, if they are at high energies). Therefore the jet should be magnetically dominated, i.e. the power carried by the jet should be mainly in the form of the Poynting flux associated to magnetic fields.

In this paper we investigate if the two claims: 1) EC favoured with respect to the SSC model, and 2) the jet is magnetically dominated (made by B08 on the basis of rather general arguments), are confirmed by detailed modelling of the SED of PKS 2155–304 with the SSC and the EC models. In particular, we consider two constraints not considered in B08: i) there is a limit on the amount of the seed external luminosity, posed by the observed flux, and ii) the predicted synchrotron flux must reproduce, or be smaller, than the observed optical/X–ray flux. We also present a new scenario, analogous to the spine/layer model, in which a compact and active region is moving within a larger jet, with a bulk Lorentz factor

⋆ E–mail: gabriele.ghisellini@brera.inaf.it

© 0000 RAS

larger then the one of the surrounding plasma. We call this version of the spine/layer model the "needle/jet" model.

2 DATA AND MODELS

The SED of PKS 2155–304 is reported in Figs. 1, 2. The shown TeV data correspond to the flare of July 28, 2006 (Aharonian et al. 2007). Red symbols are the de–absorbed fluxes, obtained with the "low SFR" model of Kneiske et al. (2004), consistent with the recent measures indicating a low value of the IR intergalactic background (Aharonian et al. 2006). Unfortunately there are no observations in other bands exactly simultaneous to the TeV flare of July 28, 2006. Therefore we do not know if the X–ray flux was also varying as rapidly, together with the TeV flux. On the other hand, PKS 2155–304 was observed on July 29–31 and several time on August, 2006 by the *Swift* satellite (see Foschini et al. 2007, hereafter F07). The X–ray and the optical data of July 30 and August 2 are shown in both Fig. 1 and Fig. 2 (see F07 for details of the analysis). Another observation by *Chandra* (partially overlapping with the first one by *Swift*) is still unpublished. PKS 2155–304 is one of the best studied extragalactic X–ray sources, and it never showed large changes of its X–ray spectral shape (unlike Mkn 501, whose synchrotron peak frequency changed by more than a factor 100). We therefore assume that the X–ray flux and slope observed on July 30 were representative of the state during the TeV flare. The other data, coming from the literature, are neither simultaneous nor close in time with the TeV data, but can give a rough representation of the entire SED, since at frequencies smaller than the synchrotron peak the flux variability is much reduced.

We will use three emission models to interpret the SED of PKS 2155–304 and in particular the rapidly variable and active TeV state observed on July 28, 2006. In all cases we will assume $\Gamma = 50$ and a source size $\sim 3 \times 10^{14}$ cm, in order to have $t_{\rm var} \sim 200$ s. The magnetic field B is tangled and homogeneous. For simplicity, the inverse Compton emission is calculated assuming a truncated scattering cross section, equal to the Thomson one if $\gamma h\nu'/m_e c^2 < 3/4$, and 0 otherwise ($\gamma m_e c^2$ is the electron energy and ν' is the photon frequency as seen in the comoving frame of the source). This mimics the real decline, with energy, of the Klein–Nishina cross section only approximately, sufficient if we are not interested to precisely describe the TeV spectrum, as in our case, but poor if we want, for instance, reconstruct the IR background through the detailed modelling of the TeV blazar spectrum.

SSC — The first model is a simple one–zone pure SSC model. As shown by Tavecchio, Maraschi & Ghisellini (1998), in this case the number of parameters characterising the model is equal to the number of observables, and there is no freedom if the frequencies and flux levels of the two peaks of the SED are known (and the variability timescale, as in our case, is given).

EC — The second model is an EC model. To fix the ideas we assume that the dominant source of seed photons is the jet beyond the TeV region. Indeed there are evidences supporting the view that the jet, soon after the location of the TeV emission, strongly decelerates. In fact, at the pc scale, VLBI data show knots moving with an apparent speed of $\beta_{\rm app} = 4.4 \pm 2.9$ (Piner & Edwards 2004, assuming the Hubble constant $H_0 = 71$ km s^{-1} Mpc^{-1}). The model parameters are chosen in order to maximise the contribution of the seed photons for the scattering process and the value of the magnetic field in the TeV emitting region. In particular we assume that the emission peaks in the mm/submm part of the spectrum, close to where the self–absorption frequency is expected.

Needle/Jet — The third model assumes that the "persistent" (e.g. varying on $\sim$hours timescales) emission is produced by a jet whose plasma moves with the standard $\Gamma = 15$ and that the variable flux originates in a small portion of the jet (a "needle"), moving at $\Gamma = 50$. The latter, being immersed in the radiation field produced by the jet, sees an enhanced radiation energy density.

In the following subsections we briefly summarise the set up of the three different models.

2.1 SSC and External Compton models

These models are described fully in Celotti & Ghisellini (2008; hereafter CG08). The observed radiation is postulated to originate in a single zone of the jet, described as a cylinder of cross sectional radius R and thickness (as seen in the comoving frame) $\Delta R' = R$.

The relativistic particles are assumed to be injected throughout the emitting volume for a finite time $t'_{\rm inj} = \Delta R'/c$. The observed (flaring) spectrum is obtained by considering the particle distribution at the end of the injection, at $t = t'_{\rm inj}$, when the emitted luminosity is maximised.

As the injection lasts for a finite timescale, not all the particles have time to cool in the time $t'_{\rm inj}$, but only those particles with energies greater than the cooling energy $\gamma_{\rm c}$. The particle distribution $N(\gamma)$ can be described as a broken power–law with a slope equal to the injection slope below $\gamma_{\rm c}$ and steeper above it. We assume a particle injection function extending from $\gamma = 1$ to $\gamma_{\rm max}$, with a broken power–law shape with slopes $\propto \gamma^{-1}$ and $\propto \gamma^{-s}$ below and above $\gamma_{\rm inj}$. The resulting shape of $N(\gamma)$ depends on the injected distribution and on the cooling time with respect to $t_{\rm inj}$.

If the cooling time is shorter than $t_{\rm inj}$ for particle energies $\gamma < \gamma_{\rm inj}$ (fast cooling regime) the resulting $N(\gamma)$ is

$$\begin{array}{lcllll} N(\gamma) & \propto & \gamma^{-(s+1)}; & \propto \gamma^{-2}; & \propto \gamma^{-1}; & \\ \gamma & > & \gamma_{\rm inj}; & \gamma_{\rm c} < \gamma < \gamma_{\rm inj}; & \gamma < \gamma_{\rm c} & (1) \end{array}$$

This is the case of our EC model. In the opposite case, only those electrons with $\gamma > \gamma_{\rm c} > \gamma_{\rm inj}$ can cool in $t_{\rm inj}$ (slow cooling regime), and we have

$$\begin{array}{lcllll} N(\gamma) & \propto & \gamma^{-(s+1)}; & \propto \gamma^{-s}; & \propto \gamma^{-1} & \\ \gamma & > & \gamma_{\rm c}; & \gamma_{\rm inj} < \gamma < \gamma_{\rm c}; & \gamma < \gamma_{\rm inj}. & (2) \end{array}$$

This is the case of our SSC model. For the EC model, the external radiation of luminosity $L_{\rm ext}$ is assumed to be produced at a distance $R_{\rm ext}$ from the black hole. Since we assume that this source is stationary with the black hole, in the comoving frame of the TeV emitting source it is seen strongly boosted and blue–shifted. The external emission is assumed to be peaked at the frequency $\nu_{\rm ext}$ and distributed as a black body (for simplicity). In the cases presented here, the random Lorentz factor of the electrons emitting at the peaks of the SED, $\gamma_{\rm peak}$, always coincides with $\gamma_{\rm inj}$.

2.2 Needle/Jet model

The model is similar to the spine/layer models described in G05 (see also Tavecchio & Ghisellini 2008). An analogous idea was also proposed in the Gamma Ry Burst field to explain the fast variability of the prompt emission (Lyutikov 2006). As in G05, we have a compact region moving faster then the rest of the jet. In G05 this was the entire "spine" of the jet, while the slower material was supposed to be a (thin) boundary layer surrounding it. Both components, in G05, had a strong radiative interplay since one sees the

radiation produced by the other relativistically boosted. Here, instead, the compact and fast region is thought as a "needle" moving throughout a larger jet. The velocity vector of the needle could even be not perfectly aligned with that of the larger jet (oblique shocks?), but for simplicity we will assume that it is. It illuminates the larger jet, but due to its larger Γ–factor the fraction of the illuminated jet is small. Consequently, we can neglect the contribution of the needle to the radiation energy density seen in the jet frame. The reverse of course is not true: the needle travels in a dense radiation field, provided by the jet emission. The idea is that the entire jet is responsible for the persistent emission of PKS 2155–304, and the "needle" is responsible for the very rapid variability.

Both the jet and the needle are filled by a tangled magnetic field and by relativistic electrons assumed to follow a smoothed broken power–law distribution extending from $\gamma_0 > 1$ to $\gamma_{\rm max}$ with slopes γ^{-n_1}, γ^{-n_2} below and above the break at $\gamma_{\rm peak}$. The normalisation of this distribution is calculated assuming that the system produces an assumed synchrotron luminosity $L'_{\rm syn}$ (as measured in the local frame), which is an input parameter of the model.

In the comoving frame of the needle the photons produced by the jet are not isotropic, but are seen aberrated. Most of them are coming from almost a single direction (opposite to the relative velocity vector). In this case the produced Compton flux is anisotropic even in the comoving frame, with more power emitted along the opposite direction of the incoming photons (i.e. for head–on scatterings). Consider also that this applies only to the Compton scatterings with photons coming from the jet, while the synchrotron and the SSC emissions are isotropic in the comoving frame. The EC radiation pattern of the needle will be more concentrated along the jet axis (in the forward direction) with respect to its synchrotron and SSC emission. The corresponding transformations are fully described in G05 and Tavecchio & Ghisellini (2008).

2.3 Jet power

Our modelling allows to derive all the quantities needed to calculate the power carried by the jet in different forms: bulk motion of cold protons and of energetic electrons, magnetic field and radiation. To each of these components there is a corresponding energy density U'_i as measured in the comoving frame of the TeV emitting source. For instance, for the electron component, $U'_i = U'_e = \int N(\gamma)\gamma m_e c^2 d\gamma$. We consider only those electrons needed to explain the emission. Since other (cold) electrons can be present, the derived power is a lower limit. For the proton component, we assume one proton per emitting electron. If the emitting leptons include electron–positron pairs, then the derived proton energy density and power are upper limits. The power is calculated through the flux across a surface perpendicular to the jet axis: $L_i \equiv \pi R^2 \Gamma^2 c U'_i$.

3 RESULTS

Fig. 1 shows the TeV data corresponding to the flare (observed and de–absorbed), together to X–ray and optical data taken a few days later (F07). The shown models are the pure SSC and the EC model, the adopted parameters are listed in Table 1. The external source of seed photons for the EC model, represented by the dotted line in Fig. 1, is assumed to be stationary with the black hole. This is likely to be not realistic, but in line with the aim to find a limit to the maximum amount of possible seed photons, in the submm band, produced externally to the TeV emitting region.

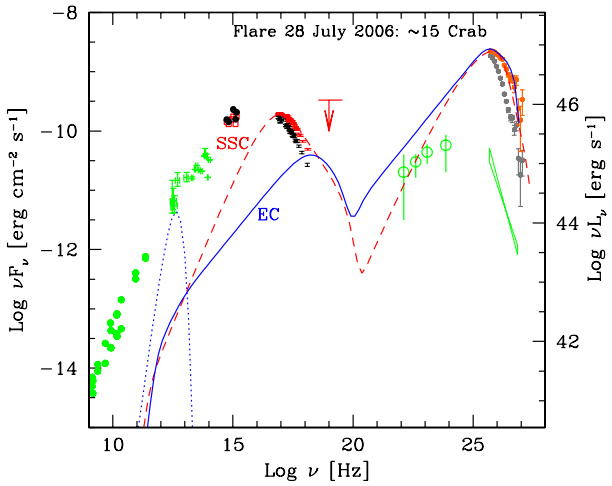


Figure 1. The SED of PKS 2155–304. Observed TeV data from H.E.S.S. (grey) correspond to the flare of 28 July 2006 (Aharonian et al. 2007). The red points report the TeV spectrum corrected for the extragalactic absorption (see text for details). X–ray and optical data are not strictly simultaneous to the TeV ones, but corresponds to 2 and 4 days later (see F07). Green symbols are archival data. We have tried to model the SED with an SSC (dashed line) and EC (solid line) assuming the parameters listed in Table 1. The dotted line corresponds to the distribution of seed photons assumed for the EC model. It has been chosen in order to maximise the high energy output of the EC emission, without overproducing the far IR observed flux.

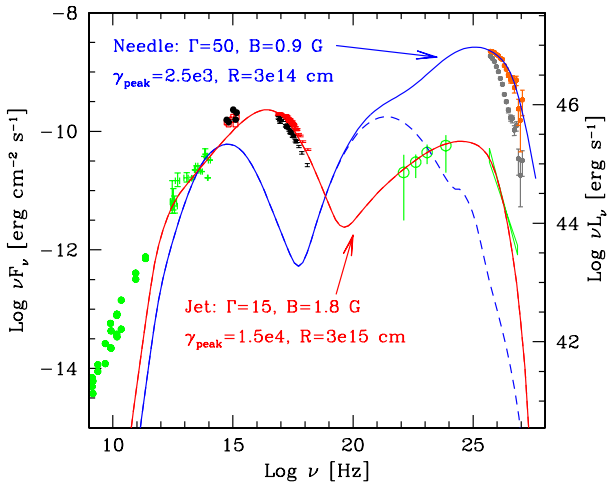


Figure 2. As in Fig 1, but the model here corresponds to a needle/jet scenario. The dashed line corresponds to the flux produced by the needle if we neglect the radiation energy density produced by the layer. The radiation energy density seen by the jet due to the needle emission is assumed to be negligible (see text).

The SSC model can satisfactorily reproduce the entire SED. For the EC model, we have choosen a solution maximizing the value of the magnetic field in the emitting region, to test the possibility to have a magnetically dominated jet. Large magnetic fields, coupled with large electron energies (necessary to emit TeV photons), yield a synchrotron peak at frequencies larger than observed. This, in turn, requires that the synchrotron flux in the EC model cannot contribute much to the low frequency peak of the SED, re-

	SSC	EC	Needle	Jet	F07	Units
Γ	50	50	50	15	30	
θ	1	1	1	1	1.7	degree
R	3.6e14	3.2e14	3e14	3e14	5e15	cm
$\Delta R'$	3.6e14	3.2e14	3e14	3e15	5e15	
B	0.58	3	0.9	1	0.27	Gauss
L'	5e40	3.5e40	—	—	1.1e42	erg s^{-1}
$L'_{\rm syn}$	—	—	3.7e39	8e40	—	erg s^{-1}
$L_{\rm ext}$	—	2e44	—	—	—	erg s^{-1}
$R_{\rm ext}$	—	3e17	—	—	—	cm
$\nu_{\rm ext}$	—	4e12	—	—	—	Hz
$\gamma_{\rm max}$	6e5	2e5	3e5	7e5	1.8e5	
$\gamma_{\rm peak}$	3e4	5e4	9e3	1.5e4	1.5e4	
γ_0	1	1	4e2	1e2	1	
n_1	—	—	2	2	—	
n_2	4.2	3.6	4.7	4.3	3.5	
$L_{\rm p}$	3.4e43	9.9e42	3.4e44	4.4e43	6.1e44	erg s^{-1}
$L_{\rm e}$	6.0e43	9.1e41	1.7e44	1.2e43	1.9e44	erg s^{-1}
$L_{\rm B}$	4.1e41	8.6e42	6.8e41	2.4e43	2.6e43	erg s^{-1}
$L_{\rm r}$	8.0e43	8.8e43	1.7e43	2.5e43	2.7e44	erg s^{-1}

Table 1. Parameters for the models used to explain the SED of PKS 2155–304 during the energetic and rapid flare of July 28, 2007. The last column (F07) reports the values of the SSC model used to fit the SED of PKS 2155–304 on the day after (i.e. July 29, 2006, when we have the simultaneous TeV and X–ray data, see F07). For all models but the last two, the Doppler factor is $\delta = 56.8$ (it is $\delta = 28$ for the "jet" and $\delta = 33.5$ for F07).

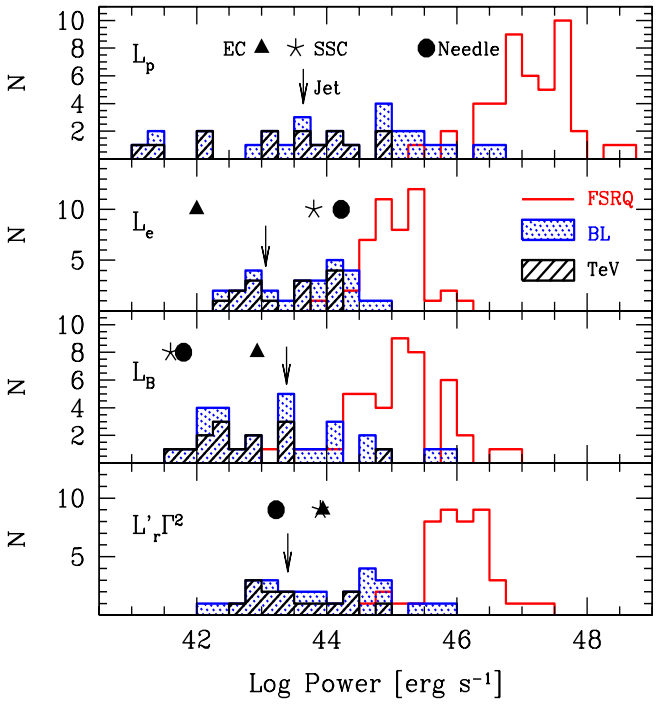


Figure 3. The power of blazar jets in bulk motion of protons ($L_{\rm p}$, assuming one proton per emitting electrons), relativistic electrons ($L_{\rm e}$), magnetic field ($L_{\rm B}$) and in radiation $L_{\rm r}$. The star, triangle, circle and arrow correspond to the values of 2155–304 during the TeV flare of 28 July 2006, whose SED has been fitted with $\Gamma = 50$ and with the SSC, the EC and the needle/jet models (see Fig. 1 and Fig. 2). These values are compared with the ones derived for a sample of blazars by CG08.

quiring another component producing the radiation below the hard X–ray band.

Fig. 2 shows the same data and the results of the needle/jet model. The dashed line shows the emission of the needle, neglecting the contribution of the radiation produced by the jet. The red solid line is the emission for the larger jet. The needle is assumed to move with $\Gamma = 50$ while the jet has $\Gamma = 15$. Note the strong enhancement of the inverse Compton flux of the needle due to the contribution of the jet radiation energy density.

Both the X–ray and the TeV flux are reproduced by the model, but the TeV flux is produced by the needle, and the X–ray flux is produced by the jet. The optical–IR flux receives comparable contributions from both. At these frequencies, the SSC and EC model have a large deficit. For the SSC model, this is due to the flatness of the electron distribution function: since the cooling time for IR emitting electrons is long, the emitting particle distribution retains the injection slope ($\propto \gamma^{-1}$) after a time $\sim R/c$. The deficit at IR frequencies of the EC model comes instead from the requirement of not overproducing the X–ray flux. Note in fact that the slope of the EC model before the synchrotron peak is softer than in the SSC model, since in this case even low energy electrons do cool in R/c, making the particle distribution $\propto \gamma^{-2}$ down to $\gamma \sim 150$.

For all models we have checked that the γ–$\gamma \to e^{\pm}$ process is not important, taking also into account (when appropriate) the target photons produced externally to the TeV emitting region.

In Fig. 3 we show the jet powers of PKS 2155–304 according to the three models, and compare these values with the ones derived for the sample of γ–ray emitting blazars studied by CG08. Note that $L_{\rm B}$ is not dominant even in the EC model, despite the fact that the enhanced radiation energy density (due to the strong boosting) allows a larger magnetic field with respect to the SSC model ($B = 3$ G vs 0.58 G, respectively). Note also that the power $L_{\rm p} + L_{\rm e}$ barely corresponds to $L_{\rm r}$ in the SSC case, and is smaller in the EC model. The needle of the needle/jet model has the largest $L_{\rm p}$, and a Poynting flux similar to the one of the SSC model. As expected, the values of the jet of the needle/jet model are comparable to the other TeV blazars considered in CG08.

In Fig. 4 we show the value $\gamma_{\rm peak}$ of PKS 2155–304 vs the comoving energy densities and jet power. The SSC and the needle/jet model give values of $\gamma_{\rm peak}$ and U' in reasonable agreement with the general trend observed for other TeV blazars, fitted with a smaller Γ. The values for the EC and spine–layer models, instead, stand clearly apart. The correlation between $\gamma_{\rm peak}$ and the jet power, $\gamma_{\rm peak} \propto L_{\rm j}^{-3/4}$, is well followed by all three models.

4 DISCUSSION

We have modelled the SED of PKS 2155–304 during the huge TeV flare of July 28, 2006 with three models, assuming always a bulk Lorentz factor $\Gamma = 50$, a size of the TeV emitting region $R \sim 3 \times 10^{14}$ cm, and a viewing angle of 1°, to account for the observed short variability timescale of the TeV flux. As mentioned in the Introduction, our aim was to check whether (as concluded by B08) in this case 1) the large Γ favours the dominance of seed photons produced externally to the jet to produce the TeV flux, and 2) the jet (or the portion of the jet) producing the variable TeV emission could be Poynting flux dominated.

The answer to 2) is negative since the Poynting flux carried by the jet is never dominating, even assuming the most favourable conditions. It is true that, in the EC case, the larger the external radiation energy density the larger the allowed magnetic field (and thus $L_{\rm B}$), but the limit posed by the SED itself to the amount of the

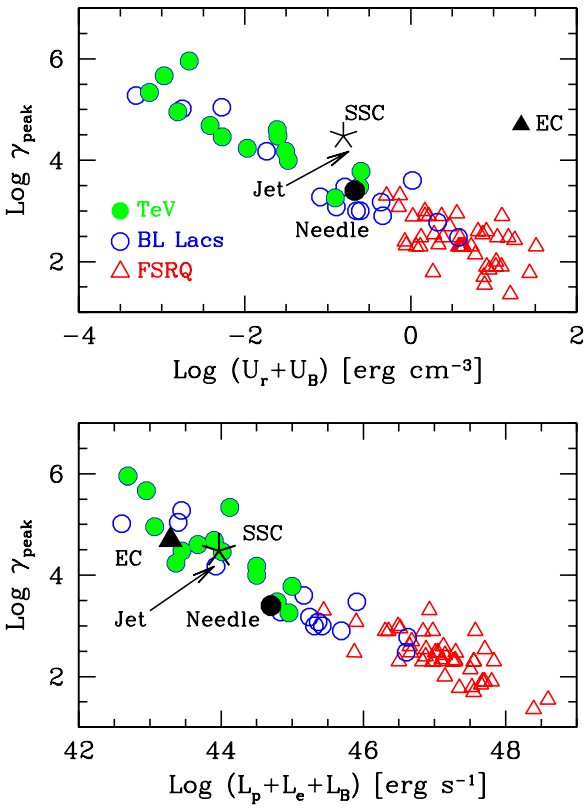


Figure 4. The random Lorentz factor, $\gamma_{\rm peak}$, of the electrons emitting at the peaks of the SED as a function of the comoving energy density (magnetic plus radiative; top panel) and the total jet power (bottom panel). The star, triangle, circle and arrow correspond to the values of PKS 2155–304 during the TeV flare of 28 July 2006, whose SED has been fitted with $\Gamma = 50$ and with the SSC, the EC and the needle/jet models (see Fig. 1 and Fig. 2). These values are compared with the values of a sample of blazars discussed in CG08.

luminosity produced externally to the TeV emitting region is also limiting the maximum value of the magnetic field.

The answer to 1) (is the external radiation important?) is more complex. In our fits the SSC model reproduces the data better than the EC model. However, this is due to the fact that we wanted to fit the high energy data and, *at the same time*, maximise the magnetic field. Allowing a *smaller* magnetic field we could obtain a better agreement with the SED. In fact the best fitting model is the needle/jet one, that can be thought as a kind of EC model, where the "external" radiation is the radiation produced by the jet itself, but externally to the needle.

In the EC case, the power carried by the jet in emitting electrons is smaller than what carried in radiation. This apparent paradox (how can the radiation have more power than the electrons producing it?) is solved recalling that in this EC model the cooling time of the electron becomes short, with the need of refreshing the electron distribution with the injection of new particles. Therefore the flow of relativistic electrons across a given jet cross sectional area underestimates the number (and the energy) of the electrons having contributed to the radiation flux. The derived $L_{\rm e}$ is therefore a lower limit.

Concerning the "blazar sequence", in the form of the relation between $\gamma_{\rm peak}$ and the energy density U' (magnetic plus radiative) seen in the comoving frame, it is well obeyed in the SSC and needle/jet case, not so for the EC model. Intriguingly, the relation between $\gamma_{\rm peak}$ and the total jet power is instead followed by all the three models.

The SSC and EC models here discussed cannot describe the "quiescent" or "persistent" state of blazars, (but in any case variable on timescale of the order of 10^4 s) since the combination of jet narrowness and the required small viewing angle cannot be reconciled with current unification schemes. One possibility is that PKS 2155–304 is unique, and the fast TeV variability will not be a general property of TeV blazars. This is unlikely, for two reasons: the first is that already another TeV blazars showed a very small $t_{\rm var}$ (i.e. Mkn 501), the other reason is that such a fast variability was observed as soon as the Cherenkov telescopes had the required sensitivity to detect it.

It may be dangerous to infer, from the ultrafast TeV variability, the general properties of a jet that can be discontinuous, either in space or in time, or both. In other words: episodes of very fast variability can be produced by "needles" of matter moving faster than average, oriented in different directions but contained in a wider cone, and occasionally pointing at the observer. Or the emitting regions are shells that corresponds to an intermittent activity of the central engine, having on average a bulk Lorentz factor that is quite large but not extreme, and occasionally going much faster (and possibly contained in a narrower cone). In the first case a "needle" would move through a region already filled with radiation (produced by the rest of the jet), and this would resemble the needle/jet model here discussed, in the second case it is likely that the emitting region would be rather external–photon–starved, and the SSC model could better describe the corresponding SED. How to distinguish the two cases? A crucial point is the UV–X–ray flux, if observed exactly simultaneously with the TeV band. If there is no sign of simultaneous fast variability, then the "needle" model is to be preferred, since the UV–X–rays could be produced by the entire jet, while the TeV flux can come from the needle. If instead both the UV–X–ray and the TeV fluxes vary together and quickly, then the SSC model is favoured.

REFERENCES

Albert J., Aliu E., Anderhub H. et al., 2007, ApJ, 669, 862

Aharonian F., Akhperjanian A.G., Razer–Bachi A.R., et al., 2006, Nature, 440, 1018

Aharonian F., Akhperjanian A.G., Razer–Bachi A.R. et al., 2007, ApJ, 664, L71

Begelman M.C., Fabian A.C. & Rees M.J., 2008, MNRAS, in press (astro–ph/0709.0540)

Celotti A & Ghisellini G., 2008, MNRAS, in press (CG08)

Dondi L. & Ghisellini G., 1995, MNRAS, 273, 583

Foschini L., Ghisellini G., Tavecchio F. et al., 2007, ApJ, 657, L81 (F07)

Georganopoulos M. & Kazanas D., 2003, ApJ, 594, L27

Ghisellini G., 1999, Astronomische Nachrichten, 320, 232

Ghisellini G., Tavecchio F. & Chiaberge M., 2005, A&A, 432, 401 (G05)

Guetta D., Ghisellini G., Lazzati D. & Celotti A., 2004, A&A, 421, 877

Kneiske T.M., Bretz T., Mannheim K., Hartmann D.H., 2004, A&A, 413, 807

Konopelko K., Mastichiadis A., Kirk J., De Jager O.C. & Stecker F.W., 2003, ApJ, 597, 851

Lytikov M., 2006, MNRAS, 369, L5

Piner G.B. & Edwards P.G., 2004, ApJ, 600, 115

Sikora M., Begelman M.C. & Rees M.J., 1994, ApJ, 421, 153

Spada, M., Ghisellini, G., Lazzati, D. & Celotti, A., 2001, MNRAS, 325, 1559

Tavecchio F., Maraschi L. & Ghisellini G., 1998, ApJ, 509, 608

Tavecchio F. & Ghisellini G., 2008, MNRAS, in press (astro–ph/0801.0593)